PCCP

Accepted Manuscript

This is an *Accepted Manuscript*, which has been through the Royal Society of Chemistry peer review process and has been accepted for publication.

Accepted Manuscripts are published online shortly after acceptance, before technical editing, formatting and proof reading. Using this free service, authors can make their results available to the community, in citable form, before we publish the edited article. We will replace this *Accepted Manuscript* with the edited and formatted *Advance Article* as soon as it is available.

You can find more information about *Accepted Manuscripts* in the Information for Authors.

Please note that technical editing may introduce minor changes to the text and/or graphics, which may alter content. The journal's standard Terms & Conditions and the Ethical guidelines still apply. In no event shall the Royal Society of Chemistry be held responsible for any errors or omissions in this *Accepted Manuscript* or any consequences arising from the use of any information it contains.

ROYAL SOCIETY OF CHEMISTRY

www.rsc.org/pccp

Journal Name

ARTICLE

Charging-induced asymmetric spin distribution in an asymmetric (9,0) carbon nanotube

Received 00th January 20xx,
Accepted 00th January 20xx

DOI: 10.1039/x0xx00000x

www.rsc.org/

Jia Wang,[a,b] Wim G. Roeterdink,[a,b] Wanrun Jiang,[a,b] Xing Dai,[a,b] Yang Gao,[a,b] Bo Wang,[a,b] Yanyu Lei,[a,b] Zhigang Wang,[a,b,*] and Rui-Qin Zhang,[c,d *]

Asymmetry in the electronic structure of low-dimensional carbon nanomaterials is important for designing molecular devices for functions such as directional transport and magnetic switching. In this paper, we use density functional theory to achieve an asymmetric spin distribution in a typical (9,0) carbon nanotube (CNT) by capping the CNT with a fullerene hemisphere at one end and saturating the dangling bonds with hydrogen atoms at the other end. The asymmetric structure facilitates obvious asymmetry in the spin distribution along the tube axis direction, with the maximum difference between the ends reaching 1.6 e/Å. More interestingly, the heterogeneity of the spin distribution can be controlled by charging the system. Increasing or decreasing the charge by 2e can reduce the maximum difference in the linear spin density along the tube axis to approximately 0.68 e/Å without changing the proportion of the total electron distribution. Further analyses of the electron density difference and the density of states reveal the loss and gain of charge and the participation of atomic orbitals at both ends. Our study characterizes the asymmetric spin distribution in a typical asymmetric carbon system and its correlation with charge at the atomic level. The results provide a strategy for controlling spin distribution for functional molecular devices through a simple charge adjustment.

Introduction

Low-dimensional nanomaterials have attracted much attention due to their unique electronic properties that facilitate potential applications in mechanical, thermal, optical, and other fields.[1-7] Compared with the geometric and electronic properties of symmetrical structures, asymmetric structures are more interesting in terms of target scattering[8], spin batteries[9], magnetic reconnection[10], and so on. Carbon nanomaterials are becoming more attractive, especially for use in pure carbon systems that are spin-polarized.[11-14] The spin polarization effects of carbon-based nanomaterials have attracted much interest for their spin valve and spin injections in molecular devices[15-17], and even in biomedical drug delivery.[18] However, few studies have looked at the design of molecular devices based on asymmetric spin distribution, even though this asymmetry is critical to targeted transport and magnetic switches.[19]

In low-dimensional carbon materials, spin polarization usually arises from localized electronic states at the edge of structures.[11, 19-24] For example, for the ground state of zigzag edge nanotubes, the spin polarization at an edge is ferromagnetic and antiferromagnetic coupled at the two zigzag edges.[11] The spin polarization is also closely related to the edge structure of nanomaterials. Graphene nanoribbons (GNRs) with zigzag edges (ZGNRs) have large spin polarization, while localized edge states are rarely seen for graphene ribbons with armchair edges (AGNRs).[20] In addition, because GNRs exhibit spin-polarized phenomena for at least three consecutive atoms at the zigzag edges[21], the number of edge atoms also has a large influence on spin polarization. Research on defects in nanomaterial structures shows that vacancies and doping also suppress the spin polarization of low-dimensional carbon materials to a certain extent.[25, 26] Theoretical simulations have also demonstrated that external electric field might have the potential to influence the spin properties and that magnetic fields can change the spin ordering on zigzag edges.[21, 27] However, existing research focuses mainly on the properties of symmetrical neutral systems.

Density Functional Theory (DFT)[28-30] is widely accepted as a suitable tool for understanding the characteristics of the geometric and electronic structures of carbon material systems.[3, 11, 19, 21, 31-35] DFT methods have been used to deal with sp^2 hybridized electronic structures in low-dimensional carbon systems with a variety of shapes, sizes[11, 20, 31] and defects, as well as the spin polarizations resulting from

[a] Institute of Atomic and Molecular Physics, Jilin University, Changchun 130012, China
[b] Jilin Provincial Key Laboratory of Applied Atomic and Molecular Spectroscopy (Jilin University), Changchun, 130012, China
[c] Department of Physics and Materials Science and Centre for Functional Photonics (CFP), City University of Hong Kong, Hong Kong SAR, China
[d] Beijing Computational Science Research Center, Beijing 100084, China
* E-mail: wangzg@jlu.edu.cn and Rui-Qin Zhang (apraz@cityu.edu.hk).
† Footnotes relating to the title and/or authors should appear here.
Electronic Supplementary Information (ESI) available: [details of any supplementary information available should be included here]. See DOI: 10.1039/x0xx00000x

Physical Chemistry Chemical Physics Accepted Manuscript

unsaturated edge structures.[21, 25, 26, 29, 31-34] Electron absorption spectra calculated using DFT methods have been shown to be in good agreement with experimental data on correlation systems.[36]

In this study, we investigate the characteristics of spin distribution using the first-principles DFT method for asymmetric nanostructures in which one end of the nanotube (9,0) is capped with a fullerene hemisphere and the dangling bonds at the other end are saturated by hydrogen atoms. We also investigate the influence of increasing or decreasing the charge in the system on spin distribution. We found that this asymmetric structure leads to an obvious asymmetry in the spin distribution in the tube axis direction. Increasing and decreasing the charge can significantly weaken the asymmetric distribution of the spin if the proportion of the electron distribution along the axial direction of the tube remains unchanged. Thus, the asymmetric structure can facilitate the control of the spin spatial distribution by increasing or decreasing the charge of the system.

Models and Computational methods

In order to build a model for study, we considered a zigzag nanotube that can be capped with a fullerene hemisphere. The (9,0) carbon nanotube (CNT), as the typical structure, is easy to synthesize experimentally and is widely used.[5, 37, 38]One end of the (9,0) CNT was capped with a C_{30} hemisphere and the dangling bonds at the other end were completely saturated by hydrogen atoms so as to construct the basic asymmetric structure of a Cap-CNT. A similar model has been employed in previous experimental[37] and theoretical[39] studies. In addition, to enable the relationship between electronic structures and the length of asymmetric nanotubes to be addressed, we considered four lengths with labels L = 1, 2, 3, and 4, denoting the number of C-C bonds of the CNT along the axis. The corresponding models with the units added on the cap are named Cap-(9,0,L). As an example, Figure 1(a) is labeled as (9,0,2) in which L=2. We then optimized all the neutral structures and the charged structures with +(-)1e or +(-)2e. We included 20 different electronic structures in total. We confirmed their stability by calculating frequencies at the same level of theory, and then performed the analysis of their electronic structures.

We used the screened exchange hybrid density functional proposed by Heyd, Scuseria, and Ernzerh (HSE06).[40, 41] It has been confirmed that the maximum Millikan spin density values calculated using HSE06 are more reasonable than those calculated by the local spin density approximation (LSDA) and the semilocal gradient corrected functional of Perdew, Burke, and Ernzerh (PBE).[21] For the HSE06 functional, the band gap is in good agreement with experimental data, with smaller mean errors than the others, more suitable for dealing with systems involving electronic localization.[34] All calculations were performed using the Gaussian 09 program[42] with the 6-31G** basis set. Spin density distribution, electron density difference, the density of states, and other data were analyzed using Multiwfn.[43]

Results and discussion

In this study, we mainly calculated and analyzed the asymmetric structures Cap-(9,0,L) with four different lengths (see Figure 1(a)). The relative energies of the ground states of the neutral structures and the structures charged at different levels for these four Cap-(9,0,L) models are shown in Figure 1(b). The optimized results show that these structures Cap-(9,0,L), which are of different lengths but have the same amount of charge, have the same spin multiplicity, indicating that the length of structure has no significant effect on spin-related properties and confirming the reliability of the model. Previous studies have revealed that the ground state of a symmetric (9,0) CNT without cap is a spin-polarized singlet[11], which is different from our system. In our system, the ground state of Cap-(9,0,L) is not the spin antiferromagnetic coupled singlet state but a high spin state quartet. This is because the open end of the nanotube's spin polarization is ferromagnetic coupled, and the spins of all the carbon atoms at the zigzag edge have the same direction (see Figure S1 in the Supporting Information). Moreover, our system contains an odd number of carbon atoms. Considering the similar electronic properties of the four models of Cap-(9,0,L), we used the model L = 2 in the discussion which follows. Choosing Cap-(9,0,2) as the typical structure not only allows a reduction of the edge effect, but also makes the conclusion more general.

Based on the optimized structures and the calculated electronic states, we carried out an analysis of the spin distribution. Interestingly, the spin polarization of Cap-(9,0,2) shows a peculiar effect for the spin distribution with increasing or decreasing charge. The spin distribution along the tube axis is also asymmetrical, as seen in Figure 2. We obtained the local integral curves of the spin density distribution along the z-axis direction according to

$$\mathbf{I_L(z)} = \int_{-\infty}^{+\infty}\int_{-\infty}^{+\infty} \boldsymbol{\rho}(\mathbf{x},\mathbf{y},\mathbf{z})\,\mathbf{dx}\,\mathbf{dy}$$

where ρ (x, y, z) is the total electron density.

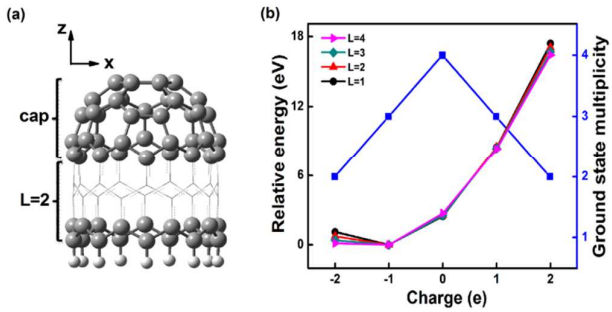

Fig. 1 (a) The geometric structure of Cap-(9,0,L). (b) The relative energies and multiplicities of the ground state for four models of Cap-(9,0,L). The Cap-(9,0,L) denotes a (9,0) CNT capped with a fullerene hemisphere at one end and the dangling bonds at the other end saturated by hydrogen atoms. L denotes the number of C-C bonds of the CNT along the axis. Here, we show only the model of L=2 as representative. In (b), the lowest energy of the structure with -1e is set as zero for reference. All the energies of the different electronic states of all 20 structures are included in the Supporting Information Table S1.

Physical Chemistry Chemical Physics Accepted Manuscript

This journal is © The Royal Society of Chemistry 20xx

We found that the difference of spin distributions at both ends along the axis was largest for the neutral structure at around 1.68 e/Å. The maximum difference of spin distribution at both ends along the axis decreases gradually as the charge of the system is changed. When the charge is +2e or -2e, the maximum difference further reduces to a minimum, nearly 0.68 e/Å. This is because the spin density distribution along the tube axis direction exhibits an oscillation feature in which spin up and down is alternated with an interval distribution. It has been verified that such oscillation behavior results from the antiferromagnetic coupling of vicinity carbon atoms.[11, 21] For neutral structures, the spin density at the open end of the nanotube, caused by the singly occupied electrons, is the largest at approximately 1.87 e/Å. Spin density decreases gradually along the tube axial direction and the spin density localized on the hexagonal of the cap is the smallest at about 0.19 e/Å. Thus, we have achieved a maximum effect for the asymmetry of spin distribution. We can adjust the trend in the spin distribution by increasing and decreasing the charge. Whether the charge increases or decreases, the spin density of the whole system decreases and does so most obviously at the open end, so that the maximum difference in the spin distribution at both ends of the axis gradually decrease.

Electronic spin density has a relationship with the number of net spins. The more net spin electrons the system carries, the greater the spin density of the system has. The ground state of the neutral structure is a quartet with three net spin electrons. The ground state of the charged structure with +(-)1e is a triplet with two net spin electrons. The ground state of the charged structure with +(-)2e is a doublet with only one net spin electron. Accordingly, we can control the magnitude of the spin density by increasing or decreasing the charge. In previous studies of CNT with both open or closed ends, similar characteristics of spin distribution have been found at both ends.[35] Our model not only reflects the asymmetric distribution of the spin, but also reveals the trend in the spin distribution in which the maximum difference in the spin at both ends of the axis decreases gradually from the neutral to the charged structure.

The electron density distribution of Cap-(9,0,2) is shown in Figure 3. It can be seen that the electron distribution with different numbers for the charge has different characteristics from the spin distribution. The increase or decrease in the charge does not greatly affect the density distribution of the electrons. In other words, the trend in the electron density hydrogen atoms is the maximum. The level of charge for the system clearly cannot control the proportion of the system electron density. This shows that increasing or decreasing the charge is capable of controlling the spin distribution.

In order to study the system that involves electron loss or gain upon the increase or decrease of charge in the neutral structure, we also obtained the electron density difference. The result is shown in Figure 4. When the charge increases or decreases, we saw that the electron density of the nanotubes changes temporarily. However, it is clear that the carbon atoms at the open end of the tube gain or lose electrons, especially when the charge of the system is +2e or -2e. This indicates that when we increase or decrease the charge, the system loses or gains electrons mainly at the open end. It is also consistent with a previous result that the variation of spin distributions at the open end for the Cap-(9,0,L) is larger when the charge of the system changes. From Figure 4(a), we saw that the value of the electron density difference between the negatively charged and the neutral structures is positive, which indicates that the system gains electrons when the charge decreases. The value of the electron density difference between the positively charged and the neutral structures is negative, indicating that the system loses electron when the

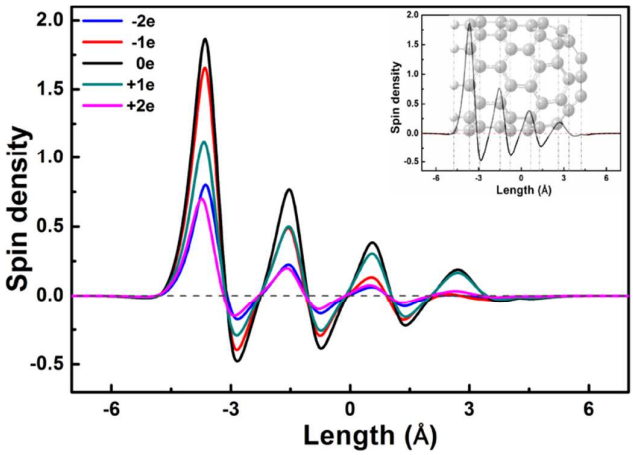

Fig. 2 The local integral curve of the spin density distribution along the tube axis (z-axis) of the neutral structure and charged structures for Cap-(9,0,2). Inset is the geometric structure and spin density, with the vertical dotted lines indicating the position of the carbon and hydrogen atoms.

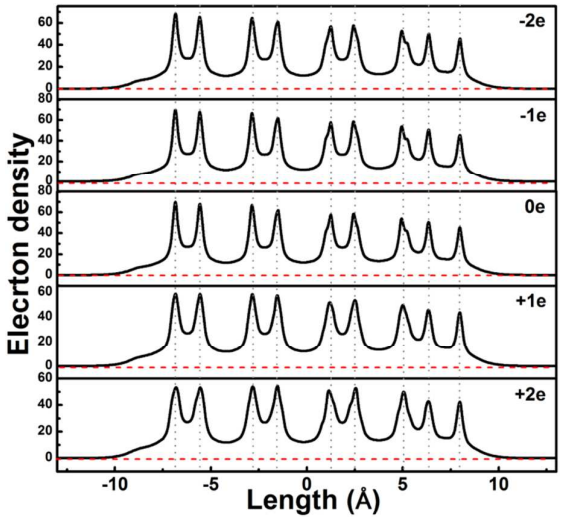

Fig. 3 The local integral curve of the electron density distribution along the tube axis (z-axis) of Cap-(9,0,2) with the neutral and charged structures. The perpendicular dotted lines indicate the position of the carbon atoms.

Physical Chemistry Chemical Physics Accepted Manuscript

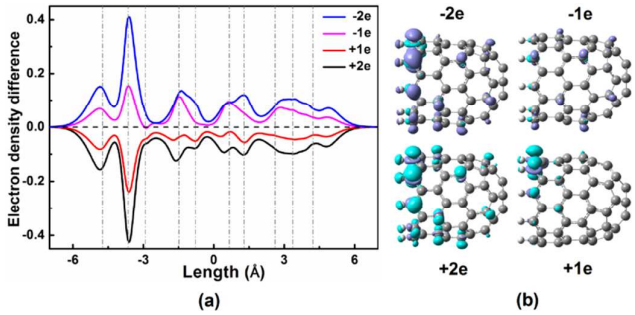

Fig. 4 The difference between the electron densities of the neutral and charged structures. (a) The local integral curve of the electron density difference along the tube axis. (b) The difference of the electron density diagram. The blue region of (b) represents the electron donor and the purple region represents the electron acceptor. +(-) n e (n=1, 2) represents the differences in electron density between cases with n charge added or reduced to the neutral structures. The isosurface value is 0.002.

charge increases. In addition, the electron density difference of the case with 2e is bigger than that with 1e, showing that the more the charge increases or decreases, the more obvious these charge transfers become.

To explore this further, we calculated the density of states[38] of these systems. As seen from the total density of states (TDOS) of Figure 5, the gap between the highest occupied molecular orbital (HOMO) and lowest unoccupied molecular orbital (LUMO) for the α electron for neutral Cap-(9,0,2) is about 1.75 eV, while the HOMO-LUMO gap for the β-electron is about 1.34 eV. The HOMO-LUMO gaps for the α-electrons for the systems with +1e or +2e are approximately 0.30 eV or 0.28 eV respectively; the HOMO-LUMO gaps for the β-electrons for the systems with +1e or +2e are nearly 1.24 eV or 0.84 eV. The HOMO-LUMO gaps of the α-electrons for the systems with -1e or -2e are about 1.63 eV or 0.43 eV, and the HOMO-LUMO gaps for the β-electrons for the systems with -1e or -2e are around 0.99 eV or 0.60 eV. It can be seen that whether the charge of the system is increasing or decreasing,

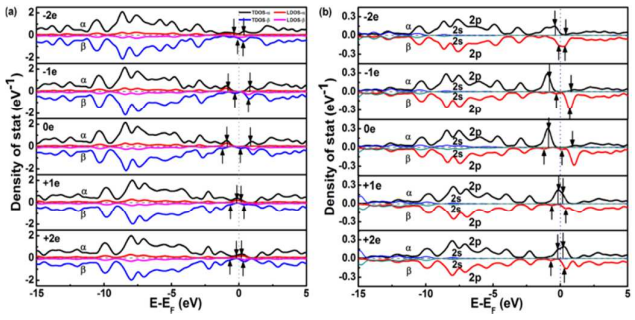

Fig. 5 Density of state of neutral and the charged structures. (a) The TDOS and LDOS of carbon atoms on the zigzag edge of (9,0,2). (b) The PDOS of the 2s and 2p orbitals of the carbon atoms on the zigzag edge. Full height and half width of the maximum (FWHM) is 0.02. The α Fermi level (indicated by vertical dashed lines) is set to zero. The short vertical arrows denote the HOMO and LUMO positions of α and β electrons.

the HOMO-LUMO gap reduces by an order of magnitude of 10^{-1}-10^{0}, which improves the conductivity of the nanotube. Compared with the neutral nanotubes of four different lengths, we found that the HOMO-LUMO gap gradually decreases by an order of magnitude of 10^{-1} with the increase of L (see Table S2 in Supporting Information).

Since the proportion of the spin density distribution on the zigzag edge is larger, we analyzed the local density of states (LDOS) of the carbon atoms on the zigzag edge, which is shown in Figure 5(a). We found that for the HOMO-α, the contribution of the carbon atoms on the zigzag edge is bigger than that of other orbitals for the neutral structure by approximately 21.90%. We then analyzed the LDOS of the charged structures. For the HOMO-α, we found that the contribution of the carbon atoms on the zigzag edge is about 77.66%, 20.56%, 25.08%, or 71.99%, which are bigger or smaller than the neutral structure, when the charge of the structure is -2e, -1e, +1e, or +2e. These results show that increasing or decreasing the charge can increase or decrease the contribution of the carbon atoms on the zigzag edges for the HOMO-α. In order to analyze the origins of the contribution of the HOMO-α of the carbon atoms on the zigzag edge, we showed the partial density of states (PDOS) of the 2s and 2p orbitals in Figure 5(b). This demonstrates that the components of HOMO-α comes mainly from the 2p orbital，rather than the 2s orbital which is mainly localized at relatively low energy region.

To facilitate comparison with possible experimental observations, we analyzed the infrared (IR) spectra and Raman activity of the ground state of Cap-(9,0,2). From Figure 6(a), an increase or decrease of the charge has a relatively large impact on the IR spectra. The peak at 883.65 cm^{-1} in the blue curve is the highest for the neutral nanotube, while those at 768.09 cm^{-1}, 873.32 cm^{-1}, 858.87 cm^{-1}, and 897.51 cm^{-1} are the highest

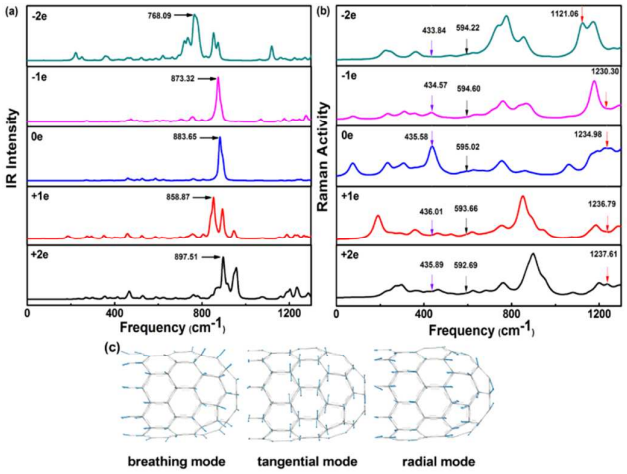

Fig. 6 (a) IR spectra and (b) Raman activity of Cap-(9,0,2) with different levels of charge. (c) Three selected modes; breathing, tangential, and radial. The arrows in Figure (a) indicate the highest peaks. The purple, black, and red arrows in Figure (b) indicate the breathing, tangential, and radial modes, respectively.

Physical Chemistry Chemical Physics Accepted Manuscript

This journal is © The Royal Society of Chemistry 20xx

for the charged structures with -2e, -1e, +1e, and +2e, respectively. These results indicate that the highest peaks for Cap-(9,0,2) with -2e, -1e, +1e are shifted to blue by an order of magnitude of 10^1-10^2 cm^{-1}, while the highest peak for Cap-(9,0,2) with +2e is shifted to red by an order of magnitude of 10^1 relative to the neutral structure. Compared with the IR spectra, Raman activity reveals three typical modes; breathing, tangential, and radial. Figure 6(c) shows these three typical patterns for the neutral Cap-(9,0,2). The breathing mode (marked by purple arrows) has a frequency of 435.58 cm^{-1}, while the breathing mode for positively and negatively charged structures are red and blue shifted, respectively, by orders of magnitude of 10^1 cm^{-1} compared with the neutral structure. The tangential mode (marked by black arrows) has a frequency of 595.02 cm^{-1}, while the tangential modes for positively and negatively charged structures are all red shifts by the order of magnitude of 10^1 cm^{-1} compared with the neutral structure. The radial mode (marked by red arrows) has a frequency of 1234.98 cm^{-1}, while the radial mode for the positively charged structure blue shifts by an order of magnitude of 10^1 cm^{-1} and for the negatively charged structure red shifts by an order of magnitude of 10^1-10^2 cm^{-1} compared with the neutral structure. Compared with previous studies of the vibrational spectra of CNTs containing defects,[25] our results are of the same order of magnitude, which again confirms the reliability of our structures.

A previous theoretical study has shown charge-induced spin polarization in α-Sexithienyl[44]. On the other hand, our research about particular metallofullerenes (EMFs) also indicated that the spin distribution has a valence dependence[45]. Besides, in neutral systems, adjusting the charge also means a control of their spin distribution. Examples include changing spin arrangements of graphene nanoribbons and relevant spin currents with the help of external electric field[21, 27]. Thus, the charge-induced adjustment of spin distribution has general significance for carbon-based nanostructures. In the experiment, the carbon nanotube was directly connected to electrodes forming a stable device when noble metal or anthracene is absorbed on it[46, 47]. Alternatively, one can achieve charge modulation by direct charge injection[44, 48, 49]. Thus, the asymmetric structure Cap-(9,0,L) may have significant potential in designing molecular devices.

Conclusions

The asymmetry of Cap-(9,0,L) results in an asymmetric spin distribution at both ends of the axis, and the differences at two ends are largest for the neutral structure at about 1.68 e/Å. Both increasing and decreasing the charge of the system can reduce the maximum difference of the spin distribution at both ends. When increasing or decreasing the charge by 2e, the maximum difference at both ends of the axis is further reduced to a minimum level of about 0.68 e/Å. The ground state of the neutral structure of the Cap-(9,0,L) is not a spin-polarized singlet but a high spin state quartet. However, on adding different numbers of charges to the system, the electron density distribution diverges from the spin density distribution, although the proportion of the former in the tube axis direction does not change significantly. Furthermore, the carbon atoms on the open end of the tube clearly gain or lose electrons, which is another reason for the appearance of higher spin density at the open end. The result of the DOS shows the contribution made by the atomic orbital by increasing or decreasing the charge. Such an increase or decrease not only shifts the highest peaks of the IR spectra to red or blue, but also induces breathing, tangential, and radial mode shifts of an order of magnitude of 10^1-10^2.

Our research provides guidance for designing asymmetric spin magnetic molecular devices at the atomic level. It has revealed a unique feature of the electron spin distribution for asymmetric structures. More importantly, our work demonstrates that control of spin polarization can be achieved by regulating the level of charge within the system, which then controls the magnetism of the structure. The asymmetry of the two ends along the axis of the structure and charge difference can make the Cap-(9,0,L) applicable in spin devices such as a spin valve and computer transistor. We hope these effects could be further controlled by external electric and magnetic fields experimentally.[27] These effects will have important applications in electromagnetic switching and directional transport.

Acknowledgements

This work was supported by the National Science Foundation of China (grant number 11374004) and the Science and Technology Development Program of Jilin Province of China (20150519021JH). Z. W. also acknowledges the Fok Ying Tung Education Foundation (142001) and High Performance Computing Center of Jilin University.

Notes and references

1 S. Iijima, *Nature*, 1991, **354**, 56-58.
2 P. Ajayan, *Chem. Rev.*, 1999, **99**, 1787-1800.
3 B. Kozinsky and N. Marzari, *Phys. Rev. Lett.*, 2006, **96**.
4 T. Yumura, D. Nozaki, K. Hirahara, S. Bandow, S. Iijima and K. Yoshizawa, *Annu. Rep. Prog. Chem., Sect. C: Phys. Chem.*, 2006, **102**, 71.
5 F. Kuemmeth, H. O. H. Churchill, P. K. Herring and C. M. Marcus, *Mater. Today*, 2010, **13**, 18-26.
6 A. K. Geim, *Science*, 2009, **324**, 1530-1534.
7 P. Avouris, Z. Chen and V. Perebeinos, *Nat. Nanotechnol.*, 2007, **2**, 605-615.
8 E. Seder, A. Biselli, S. Pisano, S. Niccolai, G. Smith, K. Joo, K. Adhikari, M. Amaryan, M. Anderson and S. A. Pereira, *Phys. Rev. Lett.*, 2015, **114**, 032001.
9 F. Chi, L.-L. Sun, J. Zheng and Y. Guo, *Phys. Lett. A*, 2015, **379**, 613-618.
10 M. Rosenberg, C. Li, W. Fox, I. Igumenshchev, F. Séguin, R. Town, J. Frenje, C. Stoeckl, V. Glebov and R. Petrasso, *Nat. Commun.*, 2015, **6**, 6190.
11 O. Hod and G. E. Scuseria, *ACS Nano*, 2008, **2**, 2243-2249.

Physical Chemistry Chemical Physics Accepted Manuscript

12 C.-K. Yang, J. Zhao and J. P. Lu, *Nano Lett.*, 2004, **4**, 561-563.
13 Z. Bullard, E. C. Girao, J. R. Owens, W. A. Shelton and V. Meunier, *Sci. Rep.*, 2015, **5**, 7634.
14 E. Durgun, R. Senger, H. Sevincli, H. Mehrez and S. Ciraci, *Phys. Rev. B*, 2006, **74**, 235413.
15 T. Taniyama, E. Wada, M. Itoh and M. Yamaguchi, *NPG Asia Mater.*, 2011, **3**, 65-73.
16 J.-W. Yoo, C.-Y. Chen, H. Jang, C. Bark, V. Prigodin, C. Eom and A. Epstein, *Nat. mater.*, 2010, **9**, 638-642.
17 W. Naber, S. Faez and W. Van Der Wiel, *J. Phys. D Appl. Phys.*, 2007, **40**, R205.
18 Z. Liu, S. Tabakman, K. Welsher and H. Dai, *Nano Res.*, 2009, **2**, 85-120.
19 B. Wu, T. Wang, Y. Feng, Z. Zhang, L. Jiang and C. Wang, *Nat. Commun.*, 2015, **6**, 6468.
20 L. Pisani, J. Chan, B. Montanari and N. Harrison, *Phys. Rev. B*, 2007, **75**, 064418.
21 O. Hod, V. Barone and G. Scuseria, *Phys. Rev. B*, 2008, **77**.
22 C. Tao, L. Jiao, O. V. Yazyev, Y. C. Chen, J. Feng, X. Zhang, R. B. Capaz, J. M. Tour, A. Zettl and S. G. Louie, *Nat. Phys.*, 2011, **7**, 616-620.
23 L. Sun, P. Wei, J. Wei, S. Sanvito and S. Hou, *J Phys-Condens. Mat.*, 2011, **23**, 425307.
24 K. Nakada, M. Fujita, G. Dresselhaus and M. S. Dresselhaus, *Phys. Rev. B* 1996, **54**, 17954-17961.
25 M. Xin, F. Wang, Y. Meng, C. Tian, M. Jin, Z. Wang and R. Zhang, *J. Phys. Chem. C* 2012, **116**, 292-297.
26 B. Huang, F. Liu, J. Wu, B.-L. Gu and W. Duan, *Phys. Rev. B*, 2008, **77**.
27 Y. W. Son, M. L. Cohen and S. G. Louie, *Nature*, 2006, **444**, 347-349.
28 R. G. Parr, *Annu. Rev. Phys. Chem.*, 1983, **34**, 631-656.
29 M. Gallo, A. Favila and D. Glossman-Mitnik, *Chem. Phys. Lett.*, 2007, **447**, 105-109.
30 X. Lu, C. Sun, F. Li and H.-M. Cheng, *Chem. Phys. Lett.*, 2008, **454**, 305-309.
31 X. Dai, C. Cheng, W. Zhang, M. Xin, P. Huai, R. Zhang and Z. Wang, *Sci. Rep.*, 2013, **3**, 1341.
32 M. Xin, X. Dai, J. Han, M. Jin, C. A. Jimenez-Cruz, D. Ding, Z. Wang and R. Zhou, *RSC Adv.*, 2014, **4**, 30074.
33 J. Han, X. Dai, Y. Gao, Y. Meng and Z. Wang, *Phys. Chem. Chem. Phys.*, 2014, **16**, 22784-22790.
34 V. Barone, O. Hod, J. E. Peralta and G. E. Scuseria, *Accounts Chem. Res.*, 2011, **44**, 269-279.
35 J. Wu and F. Hagelberg, *Phys. Rev. B*, 2009, **79**.
36 M. K. Nazeeruddin, F. De Angelis, S. Fantacci, A. Selloni, G. Viscardi, P. Liska, S. Ito, B. Takeru and M. Grätzel, *J. Am.Chem. Soc.*, 2005, **127**, 16835-16847.
37 C. Kim, B. Kim, S. Lee, C. Jo and Y. Lee, *Phys. Rev. B*, 2002, **65**, 165418.
38 R. Heyd, A. Charlier and E. McRae, *Phys. Rev. B*, 1997, **55**, 6820.
39 S.-F. Xu, G. Yuan, C. Li, Z.-J. Jia and H. Mimura, *Appl. Phys. Lett.*, 2010, **96**, 233111.
40 J. Heyd, G. E. Scuseria and M. Ernzerhof, *J. Chem. Phys.*, 2003, **118**, 8207.
41 A. V. Krukau, O. A. Vydrov, A. F. Izmaylov and G. E. Scuseria, *J. Chem. Phys.*, 2006, **125**, 224106.
42 M. J. Frisch, G. W. Trucks, H. B. Schlegel, G. E. Scuseria, M. A. Robb, J. R. Cheeseman, G. Scalmani, V. Barone, B. Mennucci, G. A. Petersson, H. Nakatsuji, M. Caricato, X. Li, H. P. Hratchian, A. F. Izmaylov, J. Bloino, G. Zheng, J. L. Sonnenberg, M. Hada, M. Ehara, K. Toyota, R. Fukuda, J. Hasegawa, M. Ishida, T. Nakajima, Y. Honda, O. Kitao, H. Nakai, T. Vreven, J. A. Montgomery Jr., J. E. Peralta, F. Ogliaro, M. J. Bearpark, J. Heyd, E. N. Brothers, K. N. Kudin, V. N. Staroverov, R. Kobayashi, J. Normand, K. Raghavachari, A. P. Rendell, J. C. Burant, S. S. Iyengar, J. Tomasi, M. Cossi, N. Rega, N. J. Millam, M. Klene, J. E. Knox, J. B. Cross, V. Bakken, C. Adamo, J. Jaramillo, R. Gomperts, R. E. Stratmann, O. Yazyev, A. J. Austin, R. Cammi, C. Pomelli, J. W. Ochterski, R. L. Martin, K. Morokuma, V. G. Zakrzewski, G. A. Voth, P. Salvador, J. J. Dannenberg, S. Dapprich, A. D. Daniels, Ö. Farkas, J. B. Foresman, J. V. Ortiz, J. Cioslowski and D. J. Fox, 2009.
43 T. Lu and F. Chen, *J. Comput. Chem.*, 2012, **33**, 580-592.
44 X. B. Yuan and J. F. Ren, *J Phys. Chem. C*, 2013, **117**, 16238-16241 .
45 X. Dai, Y. Gao, W. Jiang, Y. Lei and Z. Wang, *Phys. Chem. Chem. Phys.*, 2015, **17**, 23308-23311.
46 V. Dediu, M. Murgia, F. C. Matacotta, C. Taliani and S. Barbanera, *Solid State Commun.*, 2002, **122**, 181–184.
47 Z. Jian, J. K. Lee, W. Yue and R. W. Murray, *Nano Lett.*, 2003, **3**, 403-407.
48 C. Bittencourt, M. Hecq, A. Felten, J. J. Pireaux, J. Ghijsen, M. P. Felicissimo, P. Rudolf, W. Drube, X. Ke and G. Van Tendeloo, *Chem. Phys. Lett.*, 2008, **462**, 260-264.

Physical Chemistry Chemical Physics Accepted Manuscript

This journal is © The Royal Society of Chemistry 20xx

TOC

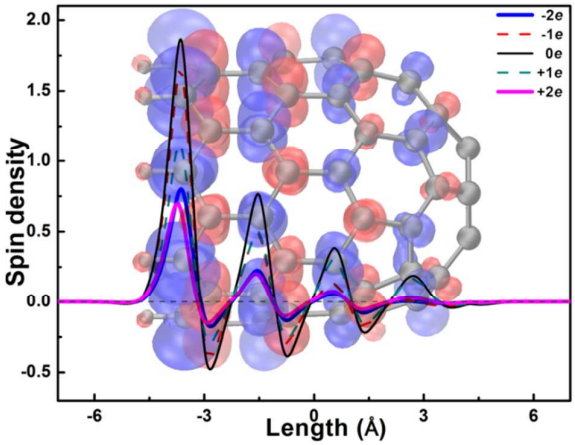

The spin distribution of asymmetric structure facilitates obvious asymmetry along the tube direction and can be controlled by charge.

Physical Chemistry Chemical Physics Accepted Manuscript